

Energy Trading and Time Scheduling for Heterogeneous Wireless-Powered and Backscattering-based IoT Networks

Ngoc-Tan Nguyen, *Student Member, IEEE*, Dinh Thai Hoang, *Member, IEEE*, Diep N. Nguyen, *Senior Member, IEEE*, Nam-Hoang Nguyen, *Member, IEEE*, Quoc-Tuan Nguyen, *Member, IEEE*, and Eryk Dutkiewicz, *Senior Member, IEEE*

Abstract—In this paper, an economic model is proposed for joint time resource allocation and energy trading between two service providers, i.e., IoT service provider (ISP) and energy service provider (ESP), in a heterogeneous IoT wireless-powered communication network. In particular, IoT devices (with various communication types and energy constraints) are assumed to belong to the ISP who collects sensing data from IoT devices for its services. Meanwhile, the ESP utilizes a power beacon to provide energy services for the ISP. A Stackelberg game model is formulated to jointly maximize the revenue of both the ISP and ESP (i.e., network throughput and energy efficiency) through investigating the energy interaction between them. Specially, the ISP leads the game by requesting an optimal energy price and service time that maximize its revenue to the ESP. Following the requested deal from the ISP, the ESP supplies an optimized transmission power which satisfies the energy demand of the ISP while maximizing its utility. To obtain the Stackelberg Equilibrium, we first derive a closed-form solution for the ESP. Then two relaxed schemes (i.e., partial or joint energy price and service time adjustments) based on *block coordinate descent* (BCD) and *convex-concave procedure* (CCCP) techniques are proposed to solve the non-convex optimization problem for the ISP. Due to the selfish behavior of both players, we investigate the inefficiency of the proposed approach by proposing two baseline scenarios, i.e., non-negotiated energy trading and social welfare scenarios, and the *Price of Anarchy* (PoA). Finally, numerical results reveal that our approach can achieve significant improvements in revenues of both providers compared with conventional transmission methods, e.g., bistatic backscatter, and harvest-then-transmit communication methods.

Index Terms—Stackelberg game, bistatic backscatter, low-power communications, heterogeneous IoT networks.

I. INTRODUCTION

Emerging Internet of Things (IoT) is a smart network which converges modern technologies to connect various smart devices to the Internet and enables information sharing and exchange among IoT devices [1]. Over the last decade, with rapid development, IoT has been applied almost everywhere such as smart city, home, agriculture, healthcare, and transportation to facilitate our lives [1]-[2]. To meet low-cost and

lightweight requirements, IoT devices are usually powered by batteries with small capacities to support their operations. However, frequent recharging/replacing batteries for a massive number of such IoT devices is ineffective because it is costly, inconvenient, and impractical in some cases (e.g., biomedical implants) [3].

A promising technology, called *Harvest-then-transmit* (HTT) [4]-[6], can be a possible solution for self-supplied IoT networks. However, due to low efficiency in harvesting energy from surrounding radio frequency (RF) signals and imperfect battery storage, energy achieved in the harvesting phase is typically low to sustain the RF communication phase on IoT devices [7]. Recently, another capable solution developed based on reflecting the incident RF signal is backscatter communications. There are three types of backscatter communications listed in [8] are monostatic [9], bistatic [10], and ambient backscatter communications [11]. Yet backscatter efficiencies of these systems are not high enough to completely replace the HTT technology. Hence, the aforementioned technologies, i.e., the HTT and backscatter communications, can be integrated to complement to each other in a hybrid system, called a wireless-powered backscatter communication (WPBC) network [12]-[16].

In a WPBC network, a wireless-powered device (WPD), e.g., an IoT device, is designed to perform either backscatter communications (i.e., passive transmissions) or transmissions using its RF circuit (i.e., active transmissions) and the energy harvested from a power beacon (PB). In order to improve the performance of the WPBC system, there is a need for a mechanism to flexibly schedule energy harvesting, passive and active transmission operations of IoT devices [13], [15], [17]. Most existing work on the WPBC optimize time allocation for IoT devices' operations under the TDM framework with the assumption of homogeneous IoT devices [12]-[16]. The experimental results show that the network throughput can be significantly improved by using this method due to absolute interference cancellation. In practice, however, various types of IoT devices with different hardware capabilities and configurations, e.g., performing backscattering or HTT or both can coexist. In such a circumstance, these devices must be taken different energy and communications constraints into account.

Game theory-based time scheduling optimization in WPBC networks has been investigated in the literature [15]-[16]. In [15], the authors propose a Stackelberg game to formulate

Ngoc-Tan Nguyen is with the School of Electrical and Data Engineering, University of Technology Sydney, Sydney, NSW 2007, Australia and JTIRC, VNU University of Engineering and Technology, Vietnam National University, Hanoi, Vietnam (e-mail: tan.nguyen@student.uts.edu.au).

D. T. Hoang, N. N. Diep, and E. Dutkiewicz are with the School of Electrical and Data Engineering, University of Technology Sydney, Sydney, NSW 2007, Australia.

N. N. Hoang, and N. Q. Tuan are with the JTIRC, VNU University of Engineering and Technology, Vietnam National University, Hanoi, Vietnam.

network throughput as the profit of the network, in which the gateway is the leader and the IoT devices are the follower. Simulation results reveal the impact of the competition on the profit of players. The authors in [16] model a single-leader-multiple-follower Stackelberg game which takes the interference's impact into account. The proposed scheme achieves a higher throughput compared with fixed transmission modes. However, a large number of IoT devices can belong to an IoT service provider (ISP) who is required to pay for energy to operate its service (e.g., a contractor that provides data collecting/monitoring services for smart cities). In such a case, the energy cost/negotiation between the ISP and an energy service provider (ESP) should be taken into account while optimizing the scheduling of IoT devices.

In this paper, our work aims to address the above by studying the self-interest interaction between the ISP and ESP (via the PB) and its implication on optimizing the energy trading and time scheduling for a heterogeneous WPBC (HWPBC) network. Specifically, we use the Stackelberg game to capture the strategic interaction between the PB and the IoT devices. Under such a game, the ISP that acts as the leader can proactively select the best energy service from the ESP by sending its energy request with a price and charging time (i.e., energy service time). The ESP modeled as the follower then finds the optimal transmission power which can maximize its benefits while meeting requirements from the ISP. A quadratic price model for energy trading [18] is developed to optimize the profit of the ESP, i.e., the follower, achieved by selling energy based on the requested price and operation time of the ISP, i.e., the leader. Thus, the optimal transmission power of the PB is derived in a close-form. In addition, the profit function of the ISP is the difference between the revenue from providing services (i.e., collecting data) and the energy cost. It is non-convex and contains multi-variables (i.e., the requested price, and operation times of the PB and IoT devices). To address the maximization problem of ISP's profit, we propose two relaxed schemes, called partial adjustment (PA) and joint adjustment (JA) of energy price and service time, that perform iterative algorithms based on the *block coordinate descent* (BCD) technique [19]. In the PA scheme, the iterative algorithm solves three sub-problems with respect to the requested price, service time of the PB, and scheduling times of the IoT devices, respectively in each its iteration. Whilst, the JA scheme splits the primary problem into two sub-problems, in which the former jointly optimize the requested price and service time of the PB, and the latter allocates the operation times for IoT devices optimally. Then, we adopt the *convex-concave procedure* (CCCP) technique [20] to address the joint sub-problem in the JA scheme. As a result, our proposed schemes can guarantee to always achieve the Stackelberg equilibrium in polynomial time. Furthermore, two baseline scenarios, i.e., non-negotiated energy trading and social welfare scenarios, and the *Price of Anarchy* (PoA) [21] ratio are proposed to evaluate the inefficiency of the proposed approach due to the selfish behaviors of both players. For performance comparison, we perform simulations to compare the revenues of both providers achieved by the proposed approach and other conventional transmission methods (i.e.,

bistatic backscatter communication mode (BBCM) [22] and HTT communication mode (HTTCM) [4]). Numerical results then verify that the proposed approach outperforms other conventional transmission methods.

The major contributions of this paper are summarized as follows:

- 1) We propose a heterogeneous WPBC network comprising of two service providers, i.e., the ISP and ESP, in which various IoT devices with diverse hardware configurations and capabilities are considered to belong the ISP.
- 2) We propose an energy trading model based on Stackelberg game where the ISP is the leader and the ESP is the follower. Two baseline scenarios, i.e., energy trading without negotiation and social welfare scenarios are presented to compare with the proposed energy trading model. In addition, the inefficiency of the proposed approach, due to selfish behaviors of both players, determined by the PoA ratio is investigated through numerical results.
- 3) Two schemes (i.e., the PA and JA schemes) performing iterative algorithms based on the BCD and CCCP techniques are proposed to maximize the revenue of the ISP which originally is a multi-variable non-convex function. Simulation results show the revenue comparison of the ISP achieved by the proposed approach and other conventional methods using both the PA and JA schemes.

The rest of the paper is organized as follows. Section II presents the system model. Section III formulates the Stackelberg game for joint energy trading and time scheduling, and two iterative algorithms are provided in Section IV to find the Stackelberg equilibrium. Section V conducts simulations to validate the theoretical derivations. Finally, Section VI concludes the paper.

II. SYSTEM MODEL

A. Network Setting

As illustrated in Fig. 1(a), we consider the HWPBC consisting of two service providers, i.e., the ISP and ESP. At the ISP, we consider three types of low-cost IoT devices with dissimilar hardware configurations that can support two functions: i.e., the BBCM and/or HTTCM. The first set of IoT devices represented by $\mathcal{A} \triangleq \{\text{AWPD}_a | \forall a = \{1, \dots, A\}\}$ is active wireless-powered IoT devices (AWPDs) that are equipped with energy harvesting and wireless transmission circuits. With this configuration, the AWPDs can operate in the HTTCM only. In addition, we denote $\mathcal{P} \triangleq \{\text{PYPD}_p | \forall p = \{1, \dots, P\}\}$ to be the set of passive wireless-powered IoT devices (PYPDs) that are designed with a backscattering circuit to perform the BBCM only. Finally, hybrid wireless-powered IoT devices (HWPDs) belonging to the set $\mathcal{H} \triangleq \{\text{HWPD}_h | \forall h = \{1, \dots, H\}\}$ are equipped with all hardware components to support both aforementioned operation modes. On the other hand, the ESP utilizes a dedicated power beacon (PB) to supply energy for the IoT devices.

The IoT service is operated over two consecutive working periods of the PB, i.e., *emitting period* β and *sleeping period* $(1 - \beta)$ as shown in Fig. 1(b). For simplicity and

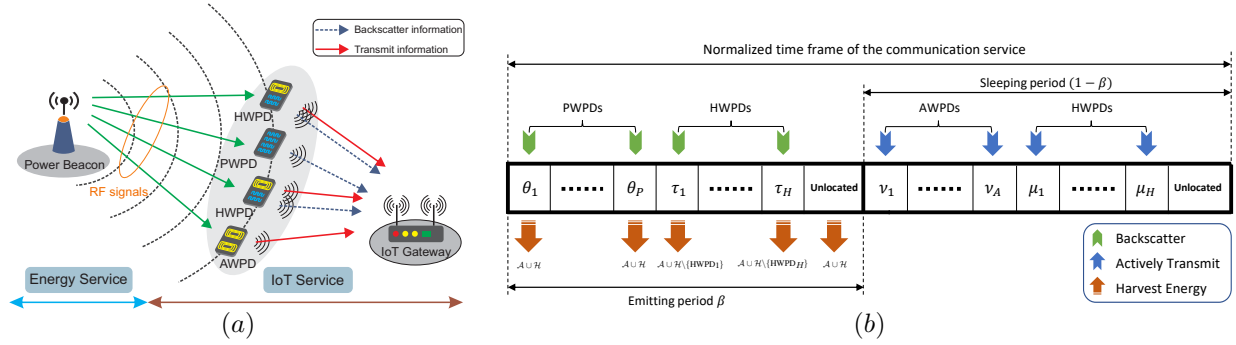


Fig. 1: (a) System model (b) Time frame of the communication service in the HWPBC network.

efficiency in time resource allocation for multiple IoT devices, the TDMA mechanism is adopted here to avoid collisions among transmissions. We denote $\theta \triangleq (\theta_1, \dots, \theta_p, \dots, \theta_P)^T$ and $\tau \triangleq (\tau_1, \dots, \tau_h, \dots, \tau_H)^T$ as the backscattering time vectors for the PWPDs and HWPDs in the emitting period of the PB, respectively. Similarly, $\nu \triangleq (\nu_1, \dots, \nu_a, \dots, \nu_A)^T$ and $\mu \triangleq (\mu_1, \dots, \mu_h, \dots, \mu_H)^T$ are the transmission time vectors for AWPDs and HWPDs in the idle period of the PB, respectively. When the PB is in the emitting period, it transmits unmodulated RF signals, and thus the IoT devices (i.e., PWPDs and HWPDs) with the capability of backscattering can passively transmit their data by leveraging such signals. Meanwhile, the AWPDs and HWPDs equipped with energy harvesting circuits can harvest energy for their active transmissions in the sleeping period of the PB. Note that, an AWPD_a can execute energy harvesting in the entire emitting period (i.e., β), while the harvesting time of an HWPD_h is $(\beta - \tau_h)$ because it must backscatter in the time slot τ_h . In the sleeping period of the PB, the AWPDs and HWPDs can perform active transmissions to deliver their data to the gateway based on the TDMA protocol.

B. Network Throughput Analysis

The network throughput (denoted by R_{sum}) of communications between the IoT devices and gateway is defined as the total information bits decoded successfully at the gateway over the two periods of the PB.

1) *Emitting period of the PB*: In this period, the IoT devices (i.e., PWPDs and HWPDs) will perform backscattering the RF signal from the PB to deliver their information. We assume that the PWPDs and HWPDs implement backscatter frequency-shift keying (FSK), or binary FSK to gain more 3 dB than the classic FSK [10]-[22]. The power beacon transmits a continuous sinusoid wave of the frequency F_c with the complex baseband equivalent as follows:

$$c(t) = \sqrt{2P_S} e^{-j(2\pi\Delta F t + \Delta\varphi)}, \quad (1)$$

where the P_S is the transmission power of the PB, ΔF and $\Delta\varphi$ are the frequency and phase offsets, respectively, between the PB and the IoT gateway.

We assume communication channels of three types of links: (1) the links from the PB to the IoT devices, (2) the links from the IoT devices to the IoT gateway, (3) the link from the PB

to the IoT gateway, suffer frequency non-selective fading (flat fading) due to the low bit rate of backscatter communications. Since the limited communication range, we consider light-of-sight (LOS) environments in this paper, thus the channel gain for the three types of links is given by:

$$g_{BD} = \frac{G_B G_D \lambda^2}{(4\pi d_{BD})^2}, g_{DG} = \frac{G_D G_G \lambda^2}{(4\pi d_{DG})^2}, g_{BG} = \frac{G_B G_G \lambda^2}{(4\pi d_{BG})^2}, \quad (2)$$

where G_B , G_D , G_G denote the antenna gains of the PB, IoT devices and IoT gateway, respectively. λ is the wavelength of the RF signal, and d_{BD} , d_{DG} , and d_{BG} are the communication distances of three aforementioned links. IoT devices are irradiated by the RF unmodulated signal $c(t)$. Then, the baseband scatter waveform at the IoT devices are written as:

$$x(t) = \gamma u_i(t) \sqrt{g_{BD}} c(t), \quad i \in \{0, 1\}, \quad (3)$$

where η is the attenuation constant of the reflected waveform depending on the backscattering efficiency. For the binary FSK modulation, we consider two distinct load values Γ_i with different rates F_i to represent bits $b_i \in \{0, 1\}$, thus the baseband backscatter FSK waveform $u_i(t)$ models the fundamental frequency component of a 50% duty cycle square waveform of frequency F_i and random initial phase $\Phi_i \in [0, 2\pi)$:

$$u_i(t) = u_0 + \frac{\Gamma_0 - \Gamma_1}{2} \frac{4}{\pi} \cos(2\pi F_i t + \Phi_i), \quad i \in \{0, 1\} \quad (4)$$

where $u_0 = (A_s - \frac{\Gamma_0 + \Gamma_1}{2})$, and A_s is a complex-valued term related to the antenna structural mode [26].

The IoT gateway receives both the RF unmodulated signal directly from the PB and the backscattered signals from the IoT devices. Thus, the received baseband signal at the IoT gateway for duration T of a single bit $b_i \in \{0, 1\}$ is given by:

$$\begin{aligned} y(t) &= \sqrt{g_{BG}} c(t) + \sqrt{g_{DG}} x(t) + n(t) \\ &= \sqrt{2P_S} \left\{ \sqrt{g_{BG}} + \gamma \sqrt{g_{BD}} \sqrt{g_{DG}} u_0 \right. \\ &\quad \left. + \gamma \sqrt{g_{BD}} \sqrt{g_{DG}} \frac{2}{\pi} (\Gamma_0 - \Gamma_1) \cos(2\pi F_i t + \Phi_i) \right\} + n(t), \end{aligned} \quad (5)$$

where $n(t)$ is the channel noise. Carrier frequency offset (CFO) and removing the DC value from the received signal $y(t)$ are carried out before the maximum-likelihood estimation (MLE) is implemented at the IoT gateway. The received signal $y(t)$ is then rewritten as follows:

$$y(t) = \gamma \sqrt{2P_S} \sqrt{g_{BD}} \sqrt{g_{DG}} \frac{2}{\pi} (\Gamma_0 - \Gamma_1) \cos(2\pi F_i t + \Phi_i) \quad (6)$$

Thus, the received power at the IoT gateway is calculated as follows:

$$P_R^{bb} = \eta^2 g_{BD} g_{DG} \frac{4}{\pi^2} (\Gamma_0 - \Gamma_1)^2 P_S \quad (7)$$

The achievable rate of backscatter communications is given by:

$$W = \Omega_B \log_2 \left(1 + \frac{\zeta P_R^{bb}}{N_0} \right) \quad (8)$$

where Ω_B is the bandwidth of the unmodulated RF signal, ζ is the performance gap reflecting real modulation, and N_0 is the power spectral density (psd) of the channel noise. We denote W_p and W_h are the achievable rates of the PWPDP_p and HWPDP_h calculated as in (8), respectively. Finally, the total throughput obtained by the AWPDPs and HWPDPs in the emitting period of the PB is determined as follows:

$$\begin{aligned} R^{bb} &= \sum_{p=1}^P W_p \theta_p + \sum_{h=1}^H W_h \tau_h \\ &= \sum_{p=1}^P \Omega_B \theta_p \log_2(1 + \kappa_p P_S) + \sum_{h=1}^H \Omega_B \tau_h \log_2(1 + \kappa_h P_S) \end{aligned} \quad (9)$$

where $\kappa_p = \zeta \eta_p^2 g_{BD,p} g_{DG,p} (\Gamma_0 - \Gamma_1)^2 \frac{4}{\pi^2 N_a^0}$ and $\kappa_h = \zeta \eta_h^2 g_{BD,h} g_{DG,h} (\Gamma_0 - \Gamma_1)^2 \frac{4}{\pi^2 N_h^0}$.

2) *Sleeping period of the PB*: As mentioned in the previous subsection, only AWPDPs and HWPDPs are able to communicate with the gateway in this period by using their RF transmission circuits. The amount of harvested energy of the AWPDP_a and HWPDP_h from the PB are calculated as follows:

$$\begin{cases} E_a = \beta P_{R,a}^B, \\ E_h = (\beta - \tau_h) P_{R,h}^B, \end{cases} \quad (10)$$

where $P_{R,a}^B = \varphi_a g_{BD,a} P_S$ and $P_{R,h}^B = \varphi_h g_{BD,h} P_S$ are the received power at the AWPDP_a and HWPDP_h from the PB, respectively [23]. P_S is the transmission power of the energy transmitter (i.e., the PB), and $\{\varphi_a, \varphi_h\}$ are the harvesting efficiency coefficients of the AWPDP_a and HWPDP_h, respectively. We consider the energy consumption by active transmissions of the AWPDPs and HWPDPs as the dominant energy consumption and ignore the energy consumed by electronic circuits. Hence, all harvested energy of the AWPDPs and HWPDPs is utilized to transmit data in the sleeping period of the PB, and the transmission power of the AWPDP_a and HWPDP_h are $P_a^t = E_a / \nu_a$ and $P_h^t = E_h / \mu_h$, respectively. Then the total throughput R^{st} achieved by active transmissions of the AWPDPs and HWPDPs in the sleeping period of the PB are determined by:

$$\begin{aligned} R^{st} &= \sum_{a=1}^A \nu_a \Omega_D \log_2 \left(1 + \frac{\zeta g_{DG,a} P_a^t}{N_a^0} \right) + \sum_{h=1}^H \mu_h \Omega_D \log_2 \left(1 + \frac{\zeta g_{DG,h} P_h^t}{N_h^0} \right) \\ &= \sum_{a=1}^A \nu_a \Omega_D \log_2 \left(1 + \delta_a \frac{\beta P_S}{\nu_a} \right) + \sum_{h=1}^H \mu_h \Omega_D \log_2 \left[1 + \delta_h \frac{(\beta - \tau_h) P_S}{\mu_h} \right], \end{aligned} \quad (11)$$

where $\delta_a = \frac{\zeta \varphi_a g_{DG,a} g_{BD,a}}{N_a^0}$ and $\delta_h = \frac{\zeta \varphi_h g_{DG,h} g_{BD,h}}{N_h^0}$. Ω_D is the bandwidth for the HTT protocol, and $\{N_a^0, N_h^0\}$ are the noise of the communication channels from the AWPDP_a and HWPDP_h to the gateway, respectively.

Finally, the network throughput (R_{sum}) of the IoT service can be determined as follows:

$$\begin{aligned} R_{sum}(\boldsymbol{\theta}, \boldsymbol{\nu}, \boldsymbol{\tau}, \boldsymbol{\mu}) &= R^{bb} + R^{st} \\ &= \sum_{p=1}^P \Omega_B \theta_p \log_2(1 + \kappa_p P_S) + \sum_{a=1}^A \nu_a \Omega_D \log_2 \left(1 + \delta_a \frac{\beta P_S}{\nu_a} \right) \\ &\quad + \sum_{h=1}^H \left\{ \Omega_B \tau_h \log_2(1 + \kappa_h P_S) + \mu_h \Omega_D \log_2 \left[1 + \delta_h \frac{(\beta - \tau_h) P_S}{\mu_h} \right] \right\}. \end{aligned} \quad (12)$$

It is modeled as the achieved profit of the communication service to jointly maximize the benefits of both service providers in the HWPBC network.

III. JOINT ENERGY TRADING AND TIME ALLOCATION BASED ON STACKELBERG GAME

Based on the system model given in the Section II, we first introduce the Stackelberg game to model the energy interaction between the ISP and ESP. Then we will present the strategic behaviors of these service providers in the following subsections.

A. Stackelberg Game-based Energy Trading

1) Game Formulation:

- **Leader payoff function:** The achievable benefit of the ISP is defined as follows:

$$U_L(p_l, \beta, \boldsymbol{\psi}) = p_r R_{sum} - p_l \beta P_S, \quad (13)$$

where p_r is the benefit per bit transmitted by IoT devices, and p_l is the energy price paid by the IoT service provider to the energy service provider. The leader maximizes its utility function U_L w.r.t. the energy price p_l , operation time β , and time scheduling $\boldsymbol{\psi} \triangleq (\boldsymbol{\theta}, \boldsymbol{\nu}, \boldsymbol{\tau}, \boldsymbol{\mu})$.

- **Follower utility function:** In this game, the PB is the follower and it optimizes its transmission power based on the requested energy price and operation time from the IoT service provider. The utility function of the follower is determined based on its profit obtained from the IoT service provider and its cost incurred during the operation time:

$$U_F(P_S) = \beta [p_l P_S - F(P_S)], \quad (14)$$

where $F(x) = a_m x^2 + b_m x$ is a quadratic function which is applied for the operation cost of the PB [18].

2) *Solution to the Stackelberg Game*: The definition of the Stackelberg equilibrium (SE) is stated as follows:

Definition 1. The optimal solution $(P_S^*, p_l^*, \beta^*, \boldsymbol{\psi}^*)$ is the Stackelberg equilibrium if the following conditions are satisfied [24]:

$$\begin{cases} U_L(P_S^*, p_l^*, \beta^*, \boldsymbol{\psi}^*) \geq U_L(P_S^*, p_l, \beta, \boldsymbol{\psi}), \\ U_F(P_S^*, p_l^*, \beta^*, \boldsymbol{\psi}^*) \geq U_F(P_S, p_l^*, \beta^*, \boldsymbol{\psi}^*). \end{cases} \quad (15)$$

To obtain the Stackelberg game solution, we adopt the backward induction technique in the two following theorems.

Theorem 1. Given a strategy of the leader (i.e., the ISP), the follower (i.e., the PB) can obtain a unique optimal P_S^* in a closed-form.

Proof: Intuitively, given a strategy (p_l, β, ψ) offered by the leader, the utility function of the follower in (14) is a quadratic function w.r.t. P_S . Thus, the unique optimal solution of P_S can be obtained as follows:

$$P_S^* = \frac{p_l - b_m}{2a_m}. \quad (16)$$

Theorem 2. *Given the follower's (i.e., the ESP) strategy P_S^* , there exists a sub-optimal solution for the leader (i.e., the ISP), and the best strategy of the ISP can be obtained by an iterative algorithm.*

Proof: Given optimal transmission power P_S^* of the follower, the leader payoff function can be rewritten as in (17). Then, the maximum profit of the leader is expressed by the strategic vector $\chi^* = (p_l^*, \beta^*, \psi^*)$:

$$\max_{(p_l, \beta, \psi)} U_L(p_l, \beta, \psi), \quad (18)$$

$$\text{s.t. } 0 \leq P_S \leq P_S^{max}, \quad (18a)$$

$$P_i^{min} \leq P_i^t \leq P_i^{max}, i \in \{a, h\}, \quad (18b)$$

$$E_i^{min} \leq E_i \leq E_i^{max}, i \in \{a, h\}, \quad (18c)$$

$$\gamma_i^{bb} \geq \gamma_i^{min}, i \in \{p, h\}, \quad (18d)$$

$$0 \leq \sum_{p=1}^P \theta_p + \sum_{h=1}^H \tau_h \leq \beta \leq 1, \forall \theta_p, \forall \tau_h \geq 0 \quad (18e)$$

$$0 \leq \sum_{a=1}^A \nu_a + \sum_{h=1}^H \mu_h \leq 1 - \beta \leq 1, \forall \nu_a, \forall \mu_h \geq 0, \quad (18f)$$

It should be noted that the transmission power of the PB, i.e., $P_S = \frac{(p_l - b_m)}{2a_m}$, must satisfy the FCC Rules [27] for unlicensed wireless equipment operating in the ISM bands as shown in the constraint (18a). For the IoT devices, the transmission power of AWPDS and HWPDS, i.e., $P_a^t = \frac{\varphi_a g_{BD,a} \beta (p_l - b_m)}{2a_m \nu_a}$, and $P_h^t = \frac{\varphi_h g_{BD,h} (\beta - \tau_h) (p_l - b_m)}{2a_m \mu_h}$, respectively, must be enough for active communication with the IoT gateway as well as under a threshold as presented in (18b). Next, the total energy harvested by the AWPDS and HWPDS in the emitting period of the PB, i.e., $E_a = \frac{\varphi_a g_{BD,a} \beta (p_l - b_m)}{2a_m}$, $E_h = \frac{\varphi_h g_{BD,h} (\beta - \tau_h) (p_l - b_m)}{2a_m}$, must be sufficient for their operations, as well as not exceed the capacity of their batteries as represented in the constraints (18c). Furthermore, the SNR at the gateway received from PWPDS and HWPDS by backscatter communications, i.e., $\gamma_p^{bb} = \frac{\kappa_p (p_l - b_m)}{2a_m}$, $\gamma_h^{bb} = \frac{\kappa_h (p_l - b_m)}{2a_m}$, must satisfy the constraints (18d) to guarantee *bit-error-rate* (BER) lower than or equal to 10^{-2} for IoT applications [ref???]. Finally, the constraints (18e)-(18f) are time constraints to impose IoT devices working on the proper periods, i.e., the PWPDS and HWPDS must backscatter RF signals in the emitting period and the AWPDS and HWPDS must perform active transmissions in the idle period of the PB.

To find the optimal solution $\chi^* = (p_l^*, \beta^*, \psi^*)$, in the next section we introduce a low-complexity iterative algorithm using *block coordinate descent* (BCD) technique [19] to address the non-convex optimization problem in (18). ■

B. Non-Negotiated Energy Trading

For comparison, we present a baseline scenario in which the ESP sends a fixed energy price to the ISP without negotiation.

Then, the ISP optimizes its profit by adjusting the transmission power and buying time demand and data transmission strategies (i.e., backscattering or active transmission). Given energy price p_l from the ESP, the achievable profit of the ISP is expressed as follows:

$$U_P(P_S, \beta, \psi) = U_T(P_S, \beta, \psi) - p_l \beta P_S, \quad (19)$$

where $U_T(P_S, \beta, \psi)$ presented in (20) is the total profit of the ISP achieved by providing data service. Then, the profit maximization of the IoT service is obtained as follows:

$$\max_{(P_S, \beta, \psi)} U_P(P_S, \beta, \psi), \quad (21)$$

$$\text{s.t. satisfy constraints (18a) - (18f),} \quad (21a)$$

It is worth noting that, in this case, the profit function of the ISP with respect to the transmission power and operation time of the PB, and the scheduling time of IoT devices can also be solved by the proposed schemes in the following section.

C. Social welfare scenario

Energy trading based on Stackelberg game formulated in section III-A captures the strategic interaction between the ISP and ESP. However, this trading strategy may lead to the performance loss of both the ISP and ESP due to the possible selfish behaviors of both players. Therefore, we propose a *social welfare* scenario in which the ISP and ESP cooperatively maximize the sum of their profits to investigate the inefficiency of the proposed approach. Mathematically, the utility function of social welfare can be formulated as below:

$$U_{SW}(P_S, \beta, \psi) = U_T(P_S, \beta, \psi) - \beta(a_m P_S^2 + b_m P_S). \quad (22)$$

Thus, the social welfare maximization problem is given by:

$$\max_{(P_S, \beta, \psi)} U_{SW}(P_S, \beta, \psi), \quad (23)$$

$$\text{s.t. satisfy constraints (18a) - (18f),} \quad (23a)$$

Similarly, the social welfare maximization problem can be also solved efficiently by the relaxed schemes proposed in the following section. To evaluate the inefficiency of the proposed approach, we use the *Price of Anarchy* (PoA) [21] which is defined as the ratio of the utility value (i.e., defined in (22)) of a worst Nash equilibrium and its maximum value. Note that, in our game, the Stackelberg equilibrium is considered as the worst Nash equilibrium. Then, the PoA ratio is expressed as below:

$$PoA = \frac{U_{SW}(\chi^*)}{\max_{(P_S, \beta, \psi)} U_{SW}(P_S, \beta, \psi)} \quad (24)$$

IV. ITERATIVE ALGORITHMS TO FIND THE STACKELBERG EQUILIBRIUM

To address the non-convex multi-variable optimization problem (18), we propose two relaxed schemes, i.e., partial adjustment (PA) and joint adjustment (JA) of the energy price and service time of the PB, which exploit the BCD technique. These schemes reduce significantly number of variables in the original optimization problem by splitting it into convex optimization sub-problems and solving them in each iteration.

$$\begin{aligned}
U_L(p_l, \beta, \psi) = p_r \left\{ \sum_{p=1}^P \Omega_B \theta_p \log_2 \left(1 + \kappa_p \frac{(p_l - b_m)}{2a_m} \right) + \sum_{a=1}^A \Omega_D \nu_a \log_2 \left[1 + \delta_a \frac{\beta (p_l - b_m)}{2\nu_a a_m} \right] \right. \\
\left. + \sum_{h=1}^H \left[\Omega_B \tau_h \log_2 \left(1 + \kappa_h \frac{(p_l - b_m)}{2a_m} \right) + \Omega_D \mu_h \log_2 \left(1 + \delta_h \frac{(\beta - \tau_h)(p_l - b_m)}{2\mu_h a_m} \right) \right] \right\} - \frac{p_l \beta (p_l - b_m)}{2a_m}. \quad (17)
\end{aligned}$$

$$U_T(P_S, \beta, \psi) = p_r \left\{ \sum_{p=1}^P \Omega_B \theta_p \log_2 (1 + \kappa_p P_S) + \sum_{a=1}^A \Omega_D \nu_a \log_2 \left(1 + \delta_a \frac{\beta P_S}{\nu_a} \right) + \sum_{h=1}^H \left[\Omega_B \tau_h \log_2 (1 + \kappa_h P_S) + \Omega_D \mu_h \log_2 \left(1 + \delta_h \frac{(\beta - \tau_h) P_S}{\mu_h} \right) \right] \right\}. \quad (20)$$

Thus, the proposed schemes expected to be a powerful tool to address the original problem efficiently are presented in the following subsections.

A. PA Scheme

This scheme performs an iterative algorithm to divide the variable tuple χ into 3 different blocks of variables, i.e., the energy price p_l , the emitting time β , and the scheduling times $\psi \triangleq (\theta, \tau, \nu, \mu)$. In particular, the algorithm starts by initializing an initial solution $\{p_l^{(0)}, \beta^{(0)}, \psi^{(0)}\}$. The following three steps are repeated until no further improvement can be obtained: (i) optimize the energy price $p_l^{(n)}$ from the last optimal output $\{p_l^{(n-1)}, \beta^{(n-1)}, \psi^{(n-1)}\}$; (ii) obtain the emitting time of the PB $\beta^{(n)}$ by keeping the $\{p_l^{(n)}, \psi^{(n-1)}\}$ fixed; (iii) find the optimal scheduling times $\psi^{(n)}$ of the IoT devices with the fixed $p_l^{(n)}$ and $\beta^{(n)}$. These steps are described in detail as the follows:

1) *Optimal Energy Price Offered for the PB*: In the first step of the algorithm loop, we obtain the optimal requested price p_l based on the optimal solution from the previous step $\{p_l^{(n-1)}, \beta^{(n-1)}, \psi^{(n-1)}\}$. It is worth noting that the time constraints in the problem (18) are eliminated because the time variables are constant and set by the previous optimal vector $\psi^{(n-1)}$. Then, the original optimization problem (18) can be transformed into:

$$\max_{p_l} G(p_l), \quad (25)$$

$$\text{s.t. } 0 \leq p_l - b_m \leq 2a_m P_S^{\max}, \quad (25a)$$

$$P_a^{\min} \leq r_{a,1} (p_l - b_m) \leq P_a^{\max}, \quad (25b)$$

$$P_h^{\min} \leq r_{h,2} (p_l - b_m) \leq P_h^{\max}, \quad (25c)$$

$$E_a^{\min} \leq r_{a,1} \nu_a^{(n-1)} (p_l - b_m) \leq E_a^{\max}, \quad (25d)$$

$$E_h^{\min} \leq r_{h,2} \mu_h^{(n-1)} (p_l - b_m) \leq E_h^{\max}, \quad (25e)$$

$$c_{p,2} (p_l - b_m) \geq \gamma_p^{\min}, \quad (25f)$$

$$c_{h,6} (p_l - b_m) \geq \gamma_h^{\min}, \quad (25g)$$

where and $c_{p,1} = p_r \Omega_B \theta_p^{(n-1)}$, $c_{p,2} = \frac{\kappa_p}{2a_m}$, $c_{a,3} = p_r \Omega_D \nu_a^{(n-1)}$, $c_{a,4} = \frac{\delta_a \beta^{(n-1)}}{2\nu_a^{(n-1)} a_m}$, $c_{h,5} = p_r \Omega_B \tau_h$, $c_{h,6} = \frac{\kappa_h}{2a_m}$, $c_{h,7} = p_r \Omega_D \mu_h^{(n-1)}$, $c_{h,8} = \frac{\delta_h (\beta^{(n-1)} - \tau_h^{(n-1)})}{2\mu_h^{(n-1)} a_m}$, $r_{a,1} = \frac{c_{a,4} N_a^a}{\zeta_{gDG,a}}$, $r_{h,2} = \frac{c_{h,8} N_h^h}{\zeta_{gDG,h}}$, ($\forall a \in \mathcal{A}, \forall h \in \mathcal{H}$).

Lemma 1. *The objective function G is a concave function w.r.t. p_l satisfying the linear constraints in (25a)-(25d), and the optimal solution for the single variable sub-problem (25) can be obtained by line search methods.*

Proof: The function $G(p_l)$ is a sum of logarithmic functions of p_l which has the form $\log_2(a_t x + b_t)$, and a quadratic function $f(p_l) = -c_9 p_l (p_l - b_m)$. Intuitively, the logarithmic function $\log_2(a_t x + b_t)$ is a concave function w.r.t. x . On the other hand, the quadratic function $f(p_l)$ is also a concave function. Thus, the objective function G is a concave function w.r.t. p_l . Since the sub-problem (25) is a single variable optimization problem which can be solved efficiently using the line search methods such as the golden section or parabolic interpolation methods. ■

2) *Optimal Emitting Time of the PB*: Similar to the sub-problem (25), the transmission power constraint of the PB, the time constraints of all IoT devices, and SNR constraints of backscatter devices are always satisfied with the fixed $\{p_l^{(n)}, \psi^{(n-1)}\}$, thus they are totally ignored. The optimal emitting time β of the PB in the n -th iteration can be obtained in the second step by solving the following sub-problem:

$$\max_{\beta} \hat{G}(\beta), \quad (27)$$

$$\text{s.t. } 0 \leq \beta \leq 1, \quad (27a)$$

$$P_a^{\min} \leq \hat{r}_{a,1} \beta \leq P_a^{\max}, \quad (27b)$$

$$P_h^{\min} \leq \hat{r}_{h,2} (\beta - \hat{c}_{h,5}) \leq P_h^{\max}, \quad (27c)$$

$$E_a^{\min} \leq \hat{r}_{a,1} \nu_a^{(n-1)} \beta \leq E_a^{\max}, \quad (27d)$$

$$E_h^{\min} \leq \hat{r}_{h,2} \mu_h^{(n-1)} (\beta - \hat{c}_{h,5}) \leq E_h^{\max}, \quad (27e)$$

where

$$\begin{aligned}
\hat{G}(\beta) = \sum_{a=1}^A \hat{c}_{a,1} \log_2 [1 + \hat{c}_{a,2} \beta] + \sum_{h=1}^H \hat{c}_{h,3} \log_2 [1 + \hat{c}_{h,4} (\beta - \hat{c}_{h,5})] \\
- \hat{c}_6 \beta + \hat{C}, \quad (28)
\end{aligned}$$

$$\begin{aligned}
\hat{C} = p_r \sum_{p=1}^P \Omega \theta_p^{(n-1)} \log_2 \left[1 + \kappa_p \frac{(p_l^{(n-1)} - b_m)}{2a_m} \right] \\
+ p_r \sum_{h=1}^H \Omega \tau_h^{(n-1)} \log_2 \left[1 + \kappa_h \frac{(p_l^{(n-1)} - b_m)}{2a_m} \right], \quad (29)
\end{aligned}$$

$$G(p_l) = \sum_{p=1}^P c_{p,1} \log_2 [1 + c_{p,2}(p_l - b_m)] + \sum_{a=1}^A c_{a,3} \log_2 [1 + c_{a,4}(p_l - b_m)] + \sum_{h=1}^H \{c_{h,5} \log_2 [1 + c_{h,6}(p_l - b_m)] + c_{h,7} \log_2 [1 + c_{h,8}(p_l - b_m)]\} - \frac{\beta^{(n-1)} p_l (p_l - b_m)}{2a_m}, \quad (26)$$

$$\begin{aligned} \hat{c}_{a,1} &= p_r \Omega_D \nu_a^{(n-1)}, \quad \hat{c}_{a,2} = \frac{\delta_a (p_l^{(n)} - b_m)}{2\nu_a^{(n-1)} a_m}, \quad \hat{c}_{h,3} = p_r \Omega_D \mu_h^{(n-1)}, \\ \hat{c}_{h,4} &= \frac{\delta_h (p_l^{(n)} - b_m)}{2\mu_h^{(n-1)} a_m}, \quad \hat{c}_{h,5} = \tau_h^{(n-1)}, \quad \hat{c}_6 = \frac{p_l^{(n)} (p_l^{(n)} - b_m)}{2a_m}, \quad \hat{r}_{a,1} = \\ &= \frac{\hat{c}_{a,2} N_0^a}{\zeta_{GDG,a}}, \quad \hat{r}_{h,2} = \frac{\hat{c}_{h,4} N_0^h}{\zeta_{GDG,h}}, \quad (\forall a \in \mathcal{A}, \forall h \in \mathcal{H}). \end{aligned}$$

Lemma 2. *The objective function \hat{G} is a concave function w.r.t. β satisfying the linear constraints in (27a)-(27c), and the optimal solution for the single variable sub-problem (27) can be obtained by line search methods.*

Proof: Following the proof of the Lemma 1, the function $\hat{G}(\beta)$ is contributed by logarithmic functions forming as $\log_2(a_t x + b_t)$ and a linear function $\hat{f}(\beta) = -\hat{c}_6 \beta$. The logarithmic function $\log_2(a_t x + b_t)$ is also concave w.r.t. x . Moreover, \hat{C} is constant with the fixed $\psi^{(n-1)}$. Thus, the objective function \hat{G} is concave w.r.t. β . Therefore, the optimal solution of the single variable sub-problem (27) can be also found efficiently by line search methods. ■

3) *Optimal Time Resource Allocation:* In the third step, we investigate the time scheduling $\psi^{(n)}$ based on the given $\{p_l^{(n)}, \beta^{(n)}\}$. The original optimization problem (18) is simplified into:

$$\max_{\psi} \tilde{G}(\psi), \quad (30)$$

$$\text{s.t. } P_a^{\min} \leq \frac{\tilde{r}_{a,1}}{\nu_a} \leq P_a^{\max}, \quad (30a)$$

$$P_h^{\min} \leq \frac{\tilde{r}_{h,2} (\tilde{c}_{h,4} - \tilde{r}_{h,5} \tau_h)}{\mu_h} \leq P_h^{\max}, \quad (30b)$$

$$E_h^{\min} \leq \tilde{r}_{h,2} (\tilde{c}_{h,4} - \tilde{c}_{h,5} \tau_h) \leq E_h^{\max}, \quad (30c)$$

$$0 \leq \sum_{p=1}^P \theta_p + \sum_{h=1}^H \tau_h \leq 1 - \beta^{(n)}, \quad \forall \theta_p, \tau_h \geq 0, \quad (30d)$$

$$0 \leq \sum_{a=1}^A \nu_a + \sum_{h=1}^H \mu_h \leq \beta^{(n)}, \quad \forall \nu_a, \mu_h \geq 0, \quad (30e)$$

where

$$\tilde{G}(\psi) = \sum_{p=1}^P \tilde{c}_{p,1} \theta_p + \sum_{a=1}^A p_r \Omega_D \nu_a \log_2 \left(1 + \frac{\tilde{c}_{a,2}}{\nu_a} \right) + \sum_{h=1}^H \left[\tilde{c}_{h,3} \tau_h + p_r \Omega_D \mu_h \log_2 \left(1 + \frac{\tilde{c}_{h,4} - \tilde{c}_{h,5} \tau_h}{\mu_h} \right) \right] + \tilde{C}, \quad (31)$$

$$\begin{aligned} \tilde{C} &= -\frac{p_l^{(n)} \beta^{(n)} (p_l^{(n)} - b_m)}{2a_m}, \quad \tilde{c}_{p,1} = p_r \Omega_B \log_2 \left[1 + \kappa_p \frac{(p_l^{(n)} - b_m)}{2a_m} \right], \quad \tilde{c}_{a,2} = \frac{\delta_a \beta^{(n)} (p_l^{(n)} - b_m)}{2a_m}, \\ \tilde{c}_{h,3} &= p_r \Omega_B \log_2 \left[1 + \kappa_h \frac{(p_l^{(n)} - b_m)}{2a_m} \right], \quad \tilde{c}_{h,4} = \frac{\delta_h \beta^{(n)} (p_l^{(n)} - b_m)}{2a_m}, \\ \tilde{c}_{h,5} &= \frac{\delta_h (p_l^{(n)} - b_m)}{2a_m}, \quad \tilde{r}_{a,1} = \frac{\tilde{c}_{3,a} N_0^a}{\zeta_{GDG,a}}, \quad \tilde{r}_{h,2} = \frac{N_0^h}{\zeta_{GDG,h}}, \end{aligned}$$

($\forall a \in \mathcal{A}, \forall h \in \mathcal{H}$). It is obvious that the SNR constraints of

backscatter devices, i.e., PVPDs and HVPDs, as well as the energy constraints for AVPDs and HVPDs are removed as they always be satisfied with the fixed $\{p_l^{(n)}, \beta^{(n)}\}$.

To obtain the optimal solution for the sub-problem (30), we have the following Lemma 3.

Lemma 3. *The objective function G_3 is a concave function w.r.t. ψ satisfying the linear constraints in (30a)-(30d), and the optimal solution for the multi-variable sub-problem (30) can be obtained by the interior-point method.*

Proof: See Appendix A. ■

4) *The overall iterative algorithm for scheme I:* Finally, the proposed iterative algorithm is summarized in the **Algorithm 1**. The convergence and computing complexity of the proposed iterative algorithm is provided in the following theorem.

Theorem 3. *For the PA scheme, the Algorithm 1 is guaranteed to converge to the SE point, and it converges in polynomial time.*

Proof: See Appendix B. ■

Algorithm 1 The iterative algorithm for the PA scheme to solve the non-convex multi-variable optimization problem in (18).

- 1: **Input:** The previous output $\{p_l^{(n-1)}, \beta^{(n-1)}, \psi^{(n-1)}\}$.
- 2: **Initialize:** $n = 1$, $\{p_l^{(0)}, \beta^{(0)}, \psi^{(0)}\}$, tolerance $\xi_1 > 0$.
- 3: **Compute:** the leader's utility $U_L(p_l^{(0)}, \beta^{(0)}, \psi^{(0)})$.
- 4: **Repeat:**
- 5: Obtain $p_l^{(n)}$ for given $\{p_l^{(n-1)}, \beta^{(n-1)}, \psi^{(n-1)}\}$ by solving (25);
- 6: Derive the optimal value $\beta^{(n)}$ with fixed $\{p_l^{(n)}, \psi^{(n-1)}\}$ by solving (27);
- 7: For given $\{p_l^{(n)}, \beta^{(n)}\}$, $\psi^{(n)}$ is obtained by solving (30);
- 8: **If:**
- 9: $|U_L(p_l^{(n)}, \beta^{(n)}, \psi^{(n)}) - U_L(p_l^{(n-1)}, \beta^{(n-1)}, \psi^{(n-1)})| < \xi_1$;
- 10: **Then:**
- 11: Set $\{p_l^*, \beta^*, \psi^*\} = \{p_l^{(n)}, \beta^{(n)}, \psi^{(n)}\}$; and terminate;
- 12: **Otherwise:**
- 13: Update $n \leftarrow n + 1$, and continue.
- 14: **Output:** The optimal solution $\chi^* = \{p_l^*, \beta^*, \psi^*\}$.

B. JA Scheme

Different to the PA scheme, we first perform a joint optimization of the energy price and service time for the PB due to their trade-off relation. After that, time scheduling for the IoT devices are obtained with the optimal value of $\{p_l, \beta\}$ in the current loop by solving the problem (30).

1) *Joint optimal energy price and service time:* With given tuple $\{p_l^{(n-1)}, \beta^{(n-1)}, \psi^{(n-1)}\}$ from the previous output, we find the joint optimal energy price and service time by solving the following sub-problem:

$$\max_{p_l, \beta} Q(p_l, \beta), \quad (32)$$

$$\text{s.t. } 0 \leq \beta \leq 1, \quad (32a)$$

$$0 \leq p_l - b_m \leq 2a_m P_S^{\max}, \quad (32b)$$

$$P_a^{\min} \leq s_{a,1} \beta (p_l - b_m) \leq P_a^{\max}, \quad (32c)$$

$$P_h^{\min} \leq s_{h,2} (\beta - \tau_h^{(n-1)}) (p_l - b_m) \leq P_h^{\max}, \quad (32d)$$

$$E_a^{\min} \leq s_{a,1} \nu_a^{(n-1)} \beta (p_l - b_m) \leq E_a^{\max}, \quad (32e)$$

$$E_h^{\min} \leq s_{h,2} \mu_h^{(n-1)} (\beta - \tau_h^{(n-1)}) (p_l - b_m) \leq E_h^{\max}, \quad (32f)$$

$$e_{p,2} (p_l - b_m) \geq \gamma_p^{\min}, e_{h,6} (p_l - b_m) \geq \gamma_h^{\min}, \quad (32g)$$

where $Q(p_l, \beta)$ is expressed in (33), and $e_{p,1} = p_r \Omega_B \theta_p^{(n-1)}$, $e_{p,2} = \frac{\kappa_p}{2a_m}$, $e_{a,3} = p_r \Omega_D \nu_a^{(n-1)}$, $e_{a,4} = \frac{\delta_a}{2\nu_a^{(n-1)} a_m}$, $e_{h,5} = p_r \Omega_B \tau_h^{(n-1)}$, $e_{h,6} = \frac{\kappa_h}{2a_m}$, $e_{h,7} = p_r \Omega_D \mu_h^{(n-1)}$, $e_{h,8} = \frac{\delta_h}{2a_m \mu_h^{(n-1)}}$, $s_{a,1} = \frac{e_{a,4} N_0^a}{\zeta_{GDG,a}}$, $s_{h,2} = \frac{e_{h,8} N_0^h}{\zeta_{GDG,h}}$, ($\forall a \in \mathcal{A}, \forall h \in \mathcal{H}$).

However, the sub-problem (32) is non-convex due to the product of $\beta(p_l - b_m)$. To address this problem, we linearise this product by defining $q_1 = \frac{1}{2}(p_l - b_m)(1 + \beta)$, $q_2 = \frac{1}{2}(p_l - b_m)(1 - \beta)$, then the problem (32) becomes:

$$\max_{q_1, q_2} \hat{Q}(q_1, q_2), \quad (34)$$

$$\text{s.t. } 0 \leq q_2 \leq q_1, \quad (34a)$$

$$0 \leq q_1 + q_2 \leq 2a_m P_S^{\max}, \quad (34b)$$

$$\frac{q_1 - q_2}{q_1 + q_2} \geq T_{bs}^{(n-1)}, \frac{2q_2}{q_1 + q_2} \geq T_{at}^{(n-1)}, \quad (34c)$$

$$P_a^{\min} \leq s_{a,1} (q_1 - q_2) \leq P_a^{\max}, \quad (34d)$$

$$P_h^{\min} \leq s_{h,2} \left[(1 - \tau_h^{(n-1)}) q_1 - (1 + \tau_h^{(n-1)}) q_2 \right] \leq P_h^{\max}, \quad (34e)$$

$$E_a^{\min} \leq s_{a,1} \nu_a^{(n-1)} (q_1 - q_2) \leq E_a^{\max}, \quad (34f)$$

$$E_h^{\min} \leq s_{h,2} \mu_h^{(n-1)} \left[(1 - \tau_h^{(n-1)}) q_1 - (1 + \tau_h^{(n-1)}) q_2 \right] \leq E_h^{\max}, \quad (34g)$$

$$e_{p,2} (q_1 + q_2) \geq \gamma_p^{\min}, e_{h,6} (q_1 + q_2) \geq \gamma_h^{\min}, \quad (34h)$$

where $\hat{Q}(q_1, q_2)$ is expressed in (35), and $T_{bs}^{(n-1)} = \sum_{p=1}^P \theta_p^{(n-1)} + \sum_{h=1}^H \tau_h^{(n-1)}$, $T_{at}^{(n-1)} = \sum_{a=1}^A \nu_a^{(n-1)} + \sum_{h=1}^H \mu_h^{(n-1)}$. Intuitively, the last term of the objective function $L(q_1, q_2)$ is convex, while other terms are concave. We define $V \triangleq \{q_1, q_2\}$ and S is the set of V satisfying (34a)-(34f), then the objective function of the problem (34) is rewritten as follows:

$$\hat{Q}(V) = Q_{ccav}(V) + Q_{cvox}(V), \quad (36)$$

where

$$Q_{cvox} = \frac{(q_2^2 + b_m q_2)}{2a_m}. \quad (38)$$

The problem (34) is the *difference-of-convex-function* (DC) programming problem, which can be solved efficiently by the

convex-concave procedure (CCCP) [20]. The core idea of the CCCP is to linearise the last term (i.e., convex function) by the first-order Taylor expansion at the current fixed point. We denote $V^{(k-1)} \triangleq \{q_1^{(k-1)}, q_2^{(k-1)}\}$ as the fixed point at the l -th iteration, then the problem (34) can be solved by the following sequential convex programming with linear constraints (34a)-(34e):

$$\begin{aligned} V^{(k)} &= \arg \max_{V \in S} \tilde{Q}(V) \\ &= \arg \max_{V \in S} \left\{ Q_{ccav}(V) + V^T \nabla Q_{cvox}(V^{(k-1)}) \right\}, \end{aligned} \quad (39)$$

where $\nabla Q_{cvox}(V^{(k-1)}) = \frac{(2q_2^{(k-1)} + b_m)}{2a_m}$ is the gradient of $Q_{cvox}(V)$ at $V^{(k-1)}$. Ultimately, $\tilde{Q}(V)$ is a convex function, thus $V^{(k)}$ can be efficiently obtained by numerical methods, such as Newton or Interior-point methods.

In general, the CCCP can start by any point within the feasible region defined by the constraints (34a)-(34e). However, we choose the initial value $V^{(0)} = \{q_1^{(0)}(p_l^{(n-1)}, \beta^{(n-1)}), q_2^{(0)}(p_l^{(n-1)}, \beta^{(n-1)})\}$ to guarantee the convergence of the proposed iterative method. The entire procedure of the CCCP algorithm is summarized in the Algorithm 2. For analysis of the convergency of the CCCP algorithm, we

Algorithm 2 The CCCP algorithm to solve the DC programming problem in (39).

- 1: **Input:** The previous result of the BCD algorithm $\{p_l^{(n-1)}, \beta^{(n-1)}, \psi^{(n-1)}\}$.
 - 2: **Initialize:** Initiate $k=1$, a tolerance $\xi_2 > 0$, and a feasible solution $V^{(0)} = \{q_1^{(0)}(p_l^{(n-1)}, \beta^{(n-1)}), q_2^{(0)}(p_l^{(n-1)}, \beta^{(n-1)})\}$.
 - 3: **Repeat:**
 - 4: Transform the problem (34) into the problem (39);
 - 5: Obtain the optimal $V^{(k-1)}$ by solving the problem (39);
 - 6: **If:**
 - 7: $|\hat{Q}(V^{(k)}) - \hat{Q}(V^{(k-1)})| < \xi_2$;
 - 8: **Then:**
 - 9: Set $V^* = V^{(k)}$; and terminate;
 - 10: **Otherwise:**
 - 11: Update $k \leftarrow k + 1$, and continue.
 - 12: **Output:** The optimal solution $V^* = \{q_1^*, q_2^*\}$.
-

state the following theorem and then prove it in Appendix C.

Theorem 4. *The Algorithm 2 utilizing the CCCP technique to solve the joint optimization problem (39). It converges to a local optimum V^* by generating a sequence of $V^{(k)}$ providing $\hat{Q}(V^{(k)}) > \hat{Q}(V^{(k-1)})$, $\forall k \geq 1$.*

2) *The overall iterative algorithm for the JA scheme:* After the implementation of the joint energy price and service time estimation, we perform time allocation for the IoT devices optimally by solving the problem (30). These steps are repeated until the stopping criterion of the algorithm is satisfied. The overall iterative algorithm for the JA scheme is summarized in the Algorithm 3. Its convergence is analyzed in the following theorem, which can be proved similarly as the Theorem 3.

$$\begin{aligned}
Q(p_l, \beta) &= \sum_{p=1}^P e_{p,1} \log_2 [1 + e_{p,2} (p_l - b_m)] + \sum_{a=1}^A e_{a,3} \log_2 [1 + e_{a,4} \beta (p_l - b_m)] \\
&+ \sum_{h=1}^H \left\{ e_{h,5} \log_2 [1 + e_{h,6} (p_l - b_m)] + e_{h,7} \log_2 \left[1 + e_{h,8} (\beta - \tau_h^{(n-1)}) (p_l - b_m) \right] \right\} - \frac{\beta p_l (p_l - b_m)}{2a_m},
\end{aligned} \tag{33}$$

$$\begin{aligned}
\hat{Q}(q_1, q_2) &= \sum_{p=1}^P e_{p,1} \log_2 [1 + e_{p,2} (q_1 + q_2)] + \sum_{a=1}^A e_{a,3} \log_2 [1 + e_{a,4} (q_1 - q_2)] \\
&+ \sum_{h=1}^H \left\{ e_{h,5} \log_2 [1 + e_{h,6} (q_1 + q_2)] + e_{h,7} \log_2 \left[1 + e_{h,8} (1 - \tau_h^{(n-1)}) q_1 - e_{h,8} (1 + \tau_h^{(n-1)}) q_2 \right] \right\} - \frac{(q_1^2 + b_m q_1)}{2a_m} + \frac{(q_2^2 + b_m q_2)}{2a_m},
\end{aligned} \tag{35}$$

$$\begin{aligned}
Q_{ccav}(V) &= \sum_{p=1}^P e_{p,1} \log_2 [1 + e_{p,2} (q_1 + q_2)] + \sum_{a=1}^A e_{a,3} \log_2 [1 + e_{a,4} (q_1 - q_2)] \\
&+ \sum_{h=1}^H \left\{ e_{h,5} \log_2 [1 + e_{h,6} (q_1 + q_2)] + e_{h,7} \log_2 \left[1 + e_{h,8} (1 - \tau_h^{(n-1)}) q_1 - e_{h,8} (1 + \tau_h^{(n-1)}) q_2 \right] \right\} - \frac{(q_1^2 + b_m q_1)}{2a_m},
\end{aligned} \tag{37}$$

Algorithm 3 The proposed iterative algorithm for the JA scheme

- 1: **Input:** The previous output $\{p_l^{(n-1)}, \beta^{(n-1)}, \psi^{(n-1)}\}$.
- 2: **Initialize:** $n = 1$, $\{p_l^{(0)}, \beta^{(0)}, \psi^{(0)}\}$, tolerance $\xi_1 > 0$.
- 3: **Compute:** the leader's utility $U_L(p_l^{(0)}, \beta^{(0)}, \psi^{(0)})$.
- 4: **Repeat:**
- 5: Obtain the joint optimal $\{p_l^{(n)}, \beta^{(n)}\}$ from the previous output $\{p_l^{(n-1)}, \beta^{(n-1)}, \psi^{(n-1)}\}$ by processing the CCCP algorithm to solve the problem (39);
- 6: Derive the optimal $\psi^{(n)}$ with fixed $\{p_l^{(n)}, \beta^{(n)}\}$ by solving the problem (27);
- 7: **If:**
- 8: $|U_L(p_l^{(n)}, \beta^{(n)}, \psi^{(n)}) - U_L(p_l^{(n-1)}, \beta^{(n-1)}, \psi^{(n-1)})| < \xi_1$;
- 9: **Then:**
- 10: Set $\{p_l^*, \beta^*, \psi^*\} = \{p_l^{(n)}, \beta^{(n)}, \psi^{(n)}\}$; and terminate;
- 11: **Otherwise:**
- 12: Update $n \leftarrow n + 1$, and continue.
- 13: **Output:** The optimal solution $\chi^* = \{p_l^*, \beta^*, \psi^*\}$.

Theorem 5. For the JA scheme, the proposed iterative Algorithm 3 converges to the SE point, and it converges in polynomial time.

Proof: Similar to the proof of the Theorem 3. ■

V. NUMERICAL RESULTS

In this section, we first investigate the inefficiency of the proposed approach, and then verify revenues of both providers in comparison with conventional transmission modes. We consider the carrier frequency of RF signals at 2.4 GHz. The bandwidth of the RF signals and the antenna gain of the PB are 10 MHz and 6 dBi, respectively. The IoT devices (i.e., AWPDS and HWPDS) have the antenna gains of 6 dBi [28]. Unless

otherwise specified, the default backscatter rate of backscatter devices is set at 10 kbps. In our setup, both the AWPDS and HWPDS have the energy harvesting and data transmission efficiency coefficients of $\varphi = 0.6$ and $\phi = 0.5$, respectively.

A. Inefficiency of the Proposed Approach

Due to the selfish behavior of players, we evaluate the inefficiency of the proposed approach by comparing with the baseline scenarios, i.e., non-negotiated energy trading and social welfare scenarios in this section. It is worth noting that, in the non-negotiated energy trading, we choose a fixed energy price at half of the maximum value. In Fig. 2, the utility functions of the ISP for the proposed approach and baseline scenarios are plotted versus the distance between the PB and the IoT devices. It can be observed that the social welfare scenario outperforms the proposed approach and the non-negotiated energy trading scenario. This is due to the cooperation between the ISP and ESP in the social welfare scenario. In addition, the profit of the non-negotiated energy trading scenario is also higher than the proposed approach. The reason is that the ISP in the non-negotiated energy trading scenario can find an optimal transmission power of the PB to maximize its revenue with the fixed energy price, whereas the ESP decides this figure in the proposed approach.

Fig. 3 shows the PoA ratio of the proposed approach using the PA and JA schemes. In both cases, the PoA ratios are small when the IoT devices are located near the PB. This is due to that Moreover, the PoA ratios are equal to zero when the distance between the PB and IoT devices is greater than 12 meters, and 18 meters in the cases of using the PA and JA schemes, respectively. It is because when the ISP and ESP are far away, the achievable profit of the ISP is lower than the energy cost. Thus, there is no success negotiation between these providers as shown in Fig. 2.

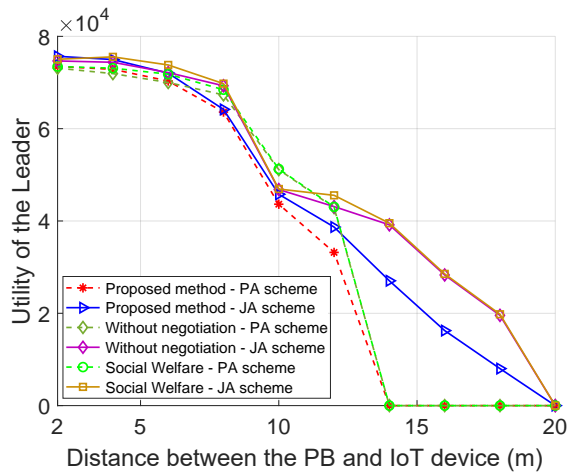


Fig. 2: Leader's payoff comparison with baseline scenarios.

B. Revenue Performance of the ISP and ESP

For performance comparison, we consider three conventional methods, i.e., the BBCM, HTTCM, and TDMA mechanism. It is worth noting that, in the TDMA mechanism, all IoT devices are allocated with identical time resources. In this case, the total backscatter time of the IoT devices accounts for a half length of the normalized time frame as illustrated in Fig. 1(b). Thus, the operation time of the PB β is fixed and equal to the total backscatter time of the IoT devices.

1) *Identical number of devices for each IoT devices set:* We first evaluate the performance of the proposed approach under the setting that the number of devices in each IoT device type are equal, (i.e., 10 devices for each IoT device type). Fig. 4 shows the variation of the leader's payoff (i.e., the ISP) as the benefit per bit transmitted (p_r) increases in the range of 0.1 to 1. The common observation is that the utilities of the ISP obtained by all methods increase as the benefit per bit transmitted increases. That is a obvious result because with more benefit gained by selling per one data bit, the ISP can purchase energy either in longer time or higher transmission power, or both, thus the profit of the ISP also increases. In particular, we first observe that the proposed approach, BBCM and HTTCM solved by scheme 2 always perform better than themselves solved by scheme 1. The reason is due to that the scheme 2 can optimize the profit of the IoT service with respect to both offered price (p_l) and the active time of the PB (β), thus it can chooses a better local optimal point than the scheme 1. Next, we also observe that the proposed method solved by scheme 2 achieves the highest profit in the considered range of p_r . In contrast, the proposed method solved by scheme 1 obtains a lower achieved profit than the TDMA mechanism when the benefit per bit transmitted is smaller than 1. Note that the scheme 1 prefers to offer a high price to buy energy rather than a long period purchasing energy, thus the optimal of this period in the scheme 1 is smaller than in the TDMA mechanism. On the other hand, the offered price has more weight than the energy purchasing time in the energy cost. For this reason, the scheme 1 might perform

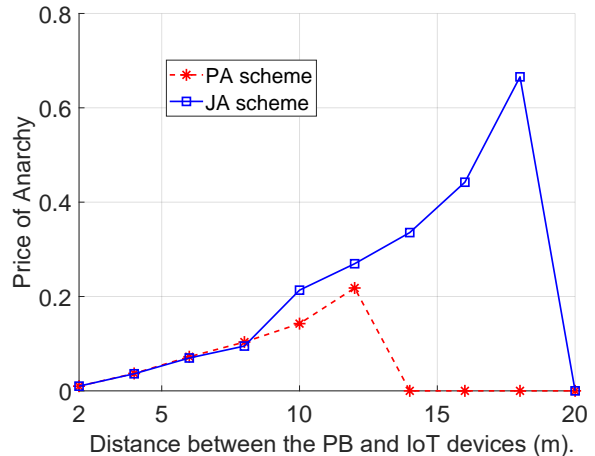


Fig. 3: Price of Anarchy.

not as good as the TDMA mechanism when the benefit per bit transmitted is under 1. Furthermore, the BBCM solved by both schemes performs much worse than other methods, in which the one solved by the scheme 2 is slightly better than the one solved by the scheme 1.

In Fig. 5, we plot the profit of the leader versus the distance between the PB and the IoT devices. At the distance of 2 meters, the profit of the ISP obtained by the BBCM using both proposed schemes are much greater than those of other approaches because transmission power of the PB is the major impact on the performance of this approach. However, its performance drastically decreases when the distance increases. By contrast, the profits of the ISP obtained by the proposed approach and HTTCM slightly reduce as the distance is smaller than 10 meters. There is no more profit for the proposed approach and HTTCM using scheme 1 when the distance is greater than or equal to 14 and 16 meters, respectively. Whilst, the profits of these approaches solved by scheme 2 are only equal to zero at the distance of 20 meters.

Next, we investigate the profit of the follower (i.e., the ESP) in Fig. 6. First, we demonstrate this profit as a quadratic function with respect to the transmission power of the PB as shown in (14). Fig. 6(a) shows the offered prices corresponding to the optimal points of the profit curve in both proposed schemes. Furthermore, as shown in the figure, scheme 1 prefers the offered price than the time purchasing energy, while the scheme 2 balances both factors. Thus, the benefit of the ESP by selling energy in the scheme 1 is much greater than the scheme 2. After applying the optimal transmission power of the PB as in (16), the profit of the ESP depends on the requested price and time purchasing energy (i.e., the operation time of the PB) announced by the IoT service as shown in Fig. 6(b). It can be seen that this profit increases linearly with the time purchasing energy and non-linearly with the offered energy price, respectively.

Fig. 7 shows the complexity of the proposed method solved by both schemes. Because both schemes take only few iterations to converge, thus in order to evaluate the computational

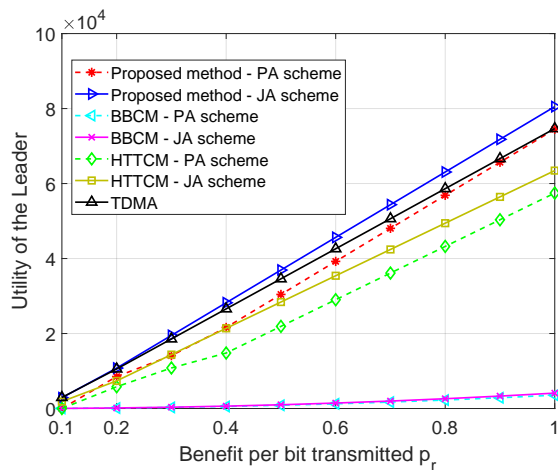


Fig. 4: Leader's payoff vs benefit per bit transmitted.

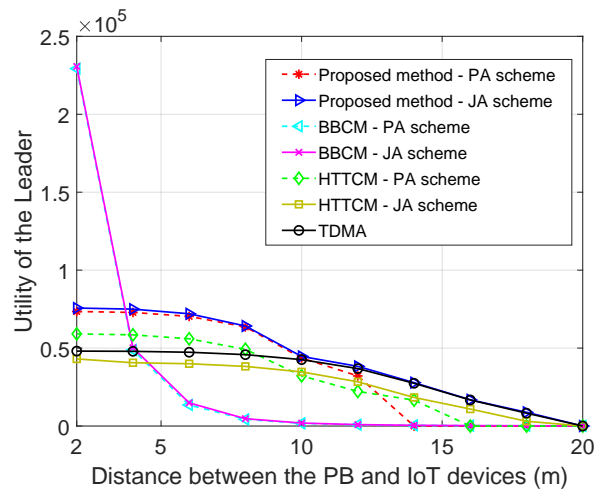


Fig. 5: Leader's payoff vs distance from the PB to the IoT devices.

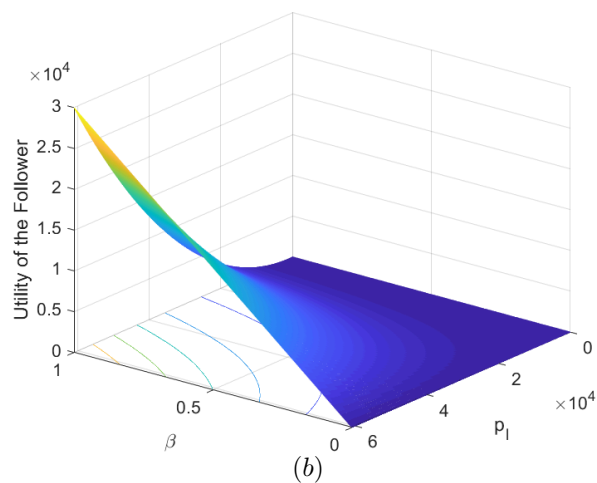
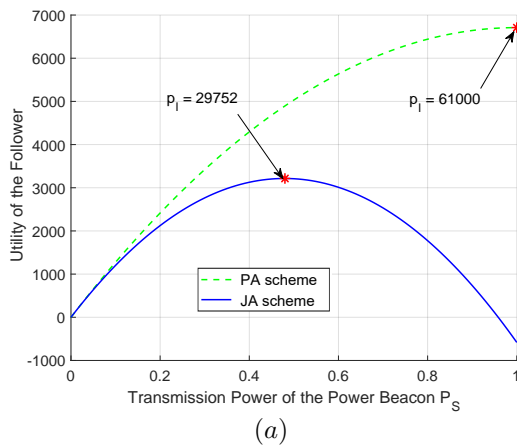


Fig. 6: Profit of the follower vs (a) transmission power of the PB, (b) offered price and time purchasing energy.

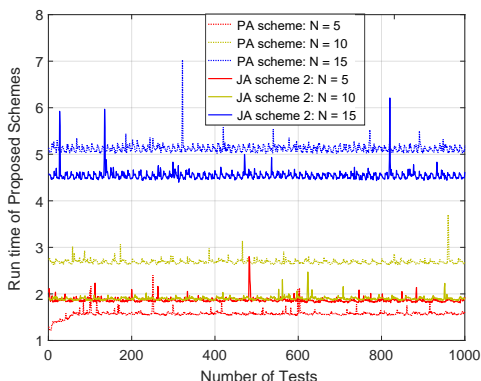


Fig. 7: Runtime of Proposed methods.

efficiency of the proposed schemes more precisely, we measure the runtime of these schemes in 1000 times with different number of IoT devices (i.e., $N = 5, N = 10, N = 15$, in which number of devices for each type is equal). In general,

we observe that the runtime of both schemes increases when the number of IoT devices increase, and the maximum runtime to solve the proposed method with 45 devices is just over 5 seconds in average by the scheme 1. In the case of small number of IoT devices (i.e., $N = 5$), the computational efficiency of the scheme 1 is better than the scheme 2. It is the result of that the scheme 2 have to run two iterative algorithms (i.e., both inner and outer iterative loops) compared to only one iterative algorithm implemented in the scheme 1. Time scheduling of the scheme 1 runs slower than the scheme 2 in all three cases because their feasible regions are different. Therefore, when the number of IoT devices increases (i.e., $N = 10, N = 15$), the scheme 2 runs faster than the scheme 1. That is due to that time scheduling accounts for the majority of the runtime of both schemes.

2) *Different number of devices for each IoT devices' set:*
We now investigate the profit of the ISP by altering the number of devices for one type from 3 to 30, while keeping these figures for other types fixed at 10. Fig. 8(a) shows a profit comparison of the ISP among approaches when varying the

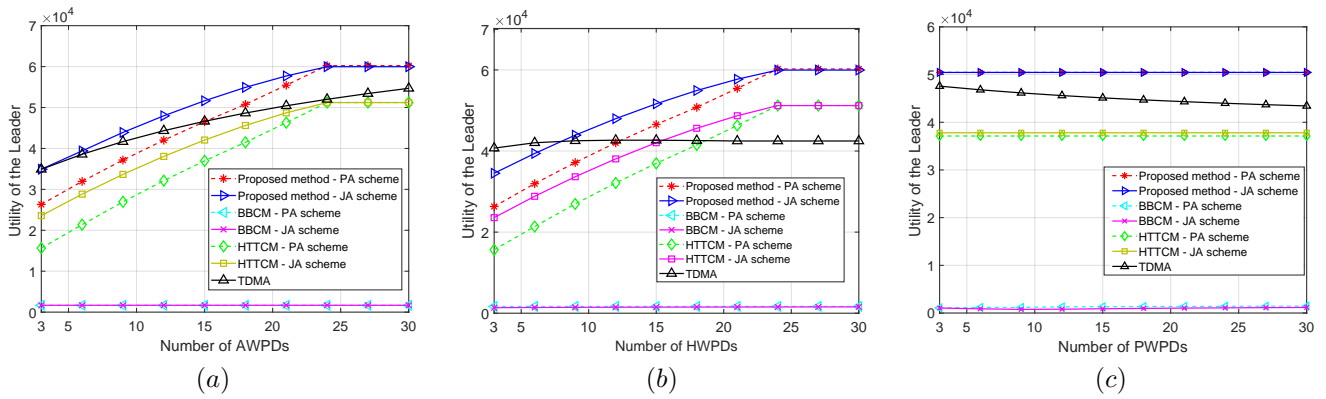


Fig. 8: Leader's payoff under different numbers of (a) HWPDs, (b) AWPDs, and (c) PWPDs.

number of AWPDs. In general observation, as the number of AWPDs is smaller than 24, the profit of the proposed method solved by scheme 2 increases and is highest compared with the others. However, when this number increases (i.e., larger than or equal to 24), the profits of the proposed method solved by both schemes are equal. There is no more profit added to the proposed method due to the power constraint violation of AWPDs. The profit of the TDMA mechanism is greater than the figure of the proposed method solved by scheme 1 as the number of AWPDs is smaller than 15. The reason is that as the number of AWPDs increases, the harvesting time reduces, thus the throughput obtained by active transmission declines. The profits of the HTTCM solved by both schemes shows the same trend but are smaller than the proposed method. These figures are also smaller than that of the TDMA mechanism. The similar trends in the profits of the proposed approach, HTTCM, and BBCM are demonstrated in Fig. 8(b). The reason is that HWPDs can perform both functions, i.e., backscattering or active transmission. By contrast, the profit of the TDMA is greater than all other approaches before it remains unchanged as the number of devices is greater than or equal to 9. In addition, as illustrated in Fig. 8(c), the increase in the number of PWPDs causes no impact on the profit of the proposed scheme due to the low level of backscatter rate. By contrast, due to sharing the time resources for PWPDs, the profit of the TDMA mechanism reduces linearly.

VI. CONCLUSION

In this paper, we have studied the Stackelberg game to maximize the profits of both service providers in heterogeneous IoT wireless-powered communication networks. The *Stackelberg Equilibrium* (SE) presented the proper price for the energy service, emitting time of the PB, and optimal scheduling times for the communication service has been obtained via the closed-form and the PA/JA schemes that exploits the BCD technique. Both the theoretical and numerical analyses have shown the convergence and computing efficiency of the iterative algorithm. Simulation results have shown that the proposed scheme always outperforms other baseline methods in terms of achieved profit of the ISP. It has also revealed that the JA scheme defeats the PA scheme in all cases.

APPENDIX A THE PROOF OF LEMMA 3

First, we consider the function $\tilde{G}(\psi)$ in (31) contributed by four terms $G_p(\theta) = \sum_{p=1}^P g_p(\theta_p)$, $G_a(\nu) = \sum_{a=1}^A g_a(\nu_a)$, and $G_h(\tau, \mu) = \sum_{h=1}^H g_h(\tau_h, \mu_h)$ and a constant \tilde{C} where

$$\begin{cases} g_p(\theta_p) &= \tilde{c}_{p,1}\theta_p, \\ g_a(\nu_a) &= p_r\Omega_D\nu_a\log_2\left(1 + \frac{\tilde{c}_{a,2}}{\nu_a}\right), \\ g_h(\tau_h, \mu_h) &= \tilde{c}_{h,3}\tau_h + p_r\Omega_D\mu_h\log_2\left[1 + \frac{\tilde{c}_{4,h} - \tilde{c}_{h,5}\tau_h}{\mu_h}\right]. \end{cases} \quad (40)$$

It is worth noting that the first term $G_p(\theta)$ are linear functions of $\theta_p, \forall p \in \{1, \dots, P\}$. The second term $G_a(\nu)$ and third term $G_h(\tau, \mu)$ are concave functions w.r.t. $\nu_a, \forall a \in \{1, \dots, A\}$ and $(\tau_h, \mu_h), \forall h \in \{1, \dots, H\}$, respectively, which are straightforward to prove by considering their Hessian matrices. Moreover, \tilde{C} is a constant with the fixed $\{p_l^{(n)}, \beta^{(n)}\}$. Finally, we can conclude that the function \tilde{G} is a concave function w.r.t. $\psi \triangleq (\theta, \nu, \tau, \mu)$ and efficiently solved by the interior-point method [29].

APPENDIX B THE PROOF OF THEOREM 3

At n -th iteration, from Lemma 1, 2, 3, we have:

$$\begin{cases} U_L(p_l^{(n)}, \beta^{(n-1)}, \psi^{(n-1)}) \geq U_L(p_l^{(n-1)}, \beta^{(n-1)}, \psi^{(n-1)}), \\ U_L(p_l^{(n)}, \beta^{(n)}, \psi^{(n-1)}) \geq U_L(p_l^{(n)}, \beta^{(n-1)}, \psi^{(n-1)}), \\ U_L(p_l^{(n)}, \beta^{(n)}, \psi^{(n)}) \geq U_L(p_l^{(n)}, \beta^{(n)}, \psi^{(n-1)}). \end{cases} \quad (41)$$

Due to the transitive property, we can obtain $U_L(p_l^{(n)}, \beta^{(n)}, \psi^{(n)}) \geq U_L(p_l^{(n-1)}, \beta^{(n-1)}, \psi^{(n-1)})$. It is worth noting that a feasible region determined by the constraints (18a)-(18f) is a compact set and always contains the output $\chi^{(n)}$, and thus the **Algorithm 1** will converge to the optimal solution χ^* . In addition, the line search and interior-point methods always find the optimal solutions of the problems (25), (27), (30) in polynomial time [30]. Then the theorem is proved.

APPENDIX C
THE PROOF OF THEOREM 4

We first prove the convergence of **Algorithm 2**. For $k > 1$, we have:

$$\begin{aligned}
\hat{G}(V^{(k)}) &\triangleq G_{ccav}(V^{(k)}) + G_{cveex}(V^{(k)}) \\
&\geq G_{ccav}(V^{(k)}) + G_{cveex}(V^{(k-1)}) \\
&\quad + (V^{(k)} - V^{(k-1)})^T \nabla G_{cveex}(V^{(k-1)}) \\
&\geq G_{ccav}(V^{(k-1)}) + (V^{(k-1)})^T \nabla G_{cveex}(V^{(k-1)}) \\
&\quad + G_{cveex}(V^{(k-1)}) - (V^{(k-1)})^T \nabla G_{cveex}(V^{(k-1)}) \\
&= G_{ccav}(V^{(k-1)}) + G_{cveex}(V^{(k-1)}) \triangleq \hat{G}(V^{(k-1)}),
\end{aligned} \tag{42}$$

where the first inequality in (42) is derived from the first order Taylor approximation of a convex function [29]:

$$G_{cveex}(V^{(k)}) \geq G_{cveex}(V^{(k-1)}) + (V^{(k)} - V^{(k-1)})^T \nabla G_{cveex}(V^{(k-1)}). \tag{43}$$

The second inequality is obtained from (39). We define S_V is the set of V satisfying the constraints (34a)-(34e). Since the S_V is a compact set and $V^{(k)}$ is always within the feasible set S_V , the CCCP algorithm will converge to V^* , i.e., $V^{(k)} = V^{(k-1)} = V^*$. Thus the **Algorithm 2** is convergence.

Next, we prove that V^* is a local optimum of the optimization problem (39). We define a constraint set $C(V) \triangleq \{C_1(V), C_2(V), \dots, C_L\}$, where L is the total number of constraints in the problem (39). Since S_V is a compact set and $\hat{G}(V)$ is concave function of V , we have the KKT condition for the optimization problem (39) as follows:

$$\begin{cases} \nabla G_{ccav}(V^{(k)}) + \nabla G_{cveex}(V^{(k-1)}) + Y^T \nabla C(V^{(k)}) = 0 \\ Y = [y_1, y_2, \dots, y_L], y_i \geq 0, y_i C_i(V^{(k)}) = 0, \forall i \end{cases} \tag{44}$$

where Y is the optimal Lagrangian variable set for $V^{(k)}$. When $V^{(k)} = V^{(k-1)} = V^*$, the above equation set can be rewritten as follows:

$$\begin{cases} \nabla G_{ccav}(V^*) + \nabla G_{cveex}(V^*) + Z^T \nabla C(V^*) = 0 \\ Z = [z_1, z_2, \dots, z_L], z_i \geq 0, z_i C_i(V^*) = 0, \forall i \end{cases} \tag{45}$$

where Z is the optimal Lagrangian variable set for V^* . That means V^* is a local optimum for the problem (39) that satisfies the KKT condition.

REFERENCES

- [1] D. Bandyopadhyay, and J. Sen, "Internet of Things: Applications and Challenges in Technology and Standardization," *Wireless Pers. Commun.*, vol. 58, no. 1, pp. 4969, 2011.
- [2] A. A. Fuqaha et al., "Internet of Things: A Survey on Enabling Technologies, Protocols, and Applications," *IEEE Commun. Surv. & Tut.*, vol. 17, no. 4, pp. 2347-2376, 2015.
- [3] D. W. K. Ng et al., "The Era of Wireless Information and Power Transfer," in *Wireless Information and Power Transfer: Theory and Practice*, Wiley, pp.1-16, 2019.
- [4] H. Ju and R. Zhang, "Throughput maximization in wireless powered communication networks," *IEEE Trans. on Wireless Commun.*, vol. 13, no. 1, pp. 418-428, Jan., 2014.
- [5] S. Lohani, R. A. Loodaricheh, E. Hossain and V. K. Bhargava, "On Multiuser Resource Allocation in Relay-Based Wireless-Powered Uplink Cellular Networks," *IEEE Trans. on Wireless Commun.*, vol. 15, no. 3, pp. 1851-1865, Mar. 2016.

- [6] A. Salem and K. A. Hamdi, "Wireless Power Transfer in Multi-Pair Two-Way AF Relaying Networks," *IEEE Transactions on Communications*, vol. 64, no. 11, pp. 4578-4591, Nov. 2016.
- [7] M. -L. Ku, W. Li, Y. Chen, and K. J. R. Liu, "Advances in energy harvesting communications: Past, present, and future challenges," *IEEE Commun. Surveys Tuts.*, vol. 18, no. 2, pp. 1384-1412, 2nd Quart., 2016.
- [8] N. Van Huynh et al., "Ambient Backscatter Communications: A Contemporary Survey," *IEEE Commun. Surv. & Tut.*, vol. 20, no. 4, pp. 2889-2922, 2018.
- [9] A. Bletsas, S. Siachalou and J. N. Sahalos, "Anti-collision backscatter sensor networks," *IEEE Transactions on Wireless Communications*, vol. 8, no. 10, pp. 5018-5029, Oct. 2009.
- [10] J. Kimionis, A. Bletsas and J. N. Sahalos, "Increased Range Bistatic Scatter Radio," in *IEEE Transactions on Communications*, vol. 62, no. 3, pp. 1091-1104, March 2014.
- [11] V. Liu et al., "Ambient backscatter: Wireless communication out of thin air," in *Proc. ACM SIGCOMM*, Hong Kong, Aug. 2013, pp. 3950.
- [12] S. Gong et al., "Backscatter Relay Communications Powered by Wireless Energy Beamforming," *IEEE Trans. on Commun.*, vol. 66, no. 7, pp. 3187-3200, Jul., 2018.
- [13] P. Wang et al., "Optimal Resource Allocation for Secure Multi-User Wireless Powered Backscatter Communication with Artificial Noise," *IEEE INFOCOM*, pp. 460-468, France, 2019.
- [14] B. Lyu, Z. Yang, G. Gui, and Y. Feng, "Wireless powered communication networks assisted by backscatter communication," *IEEE Access*, vol. 5, pp. 7254-7262, Mar., 2017.
- [15] D. T. Hoang et al., "Overlay RF-powered backscatter cognitive radio networks: A game theoretic approach," *IEEE Inter. Conf. on Commun.*, pp. 1-6, Paris, 2017.
- [16] W. Wang et al., "Stackelberg Game for Distributed Time Scheduling in RF-Powered Backscatter Cognitive Radio Networks," in *IEEE Trans. on Wireless Commun.*, vol. 17, no. 8, pp. 5606-5622, Aug., 2018.
- [17] W. Chen, C. Li, S. Gong, L. Gao, and J. Xu, "Joint transmission scheduling and power allocation in wirelessly powered hybrid radio networks," in *Proc. IEEE ICNC, Honolulu*, HI, USA, Feb. 2019, pp. 515519.
- [18] A. Mohsenian-Rad et al., "Autonomous demand-side management based on game-theoretic energy consumption scheduling for the future smart grid," *IEEE Trans. on Smart Grid*, vol. 1, no. 3, pp. 320-331, 2010.
- [19] P. Tseng, "Convergence of a block coordinate descent method for nondifferentiable minimization," *Jour. Optim. Theory Appl.*, vol. 109, no. 3, pp. 475494, 2001.
- [20] A. L. Yuille and A. Rangarajan, "The concave-convex procedure (CCCP)," *Proc. Adv. Neural Inf. Process. Syst.*, , pp. 10331040, Apr. 2001.
- [21] T. Roughgarden, "Intrinsic robustness of the price of anarchy," *J. ACM*, vol. 62, no. 5, Nov. 2015, Art. no. 32.
- [22] N. F. Hilliard, P. N. Alevizos and A. Bletsas, "Coherent Detection and Channel Coding for Bistatic Scatter Radio Sensor Networking," *IEEE Trans. on Commun.*, vol. 63, no. 5, pp. 1798-1810, May, 2015.
- [23] C. A. Balanis, *Antenna Theory: Analysis and Design*. NY, Wiley, 2012.
- [24] D. Fudenberg, J. Tirole, *Game Theory*, MIT Press, 1991.
- [25] P. N. Alevizos, K. Tountas and A. Bletsas, "Multistatic Scatter Radio Sensor Networks for Extended Coverage," in *IEEE Transactions on Wireless Communications*, vol. 17, no. 7, pp. 4522-4535, July 2018.
- [26] A. Bletsas, A. G. Dimitriou, and J. N. Sahalos, "Improving backscatter radio tag efficiency," *IEEE Trans. Microwave Theory Tech.*, vol. 58, no. 6, pp. 15021509, Jun. 2010
- [27] FCC Rules for RF devices, part 15, Oct 2018. Available at: <http://afar.net/tutorials/fcc-rules/>.
- [28] D. Y. Kim and D. I. Kim, "Reverse-link interrogation range of a UHF MIMO-RFID system in Nakagami-m fading channels," *IEEE Trans. on Indus. Electronics*, vol. 57, no. 4, pp. 1468-1477, Apr., 2010.
- [29] S. Boyd and L. Vandenberghe, *Convex Optimization*, Cambridge, U.K.: Cambridge Univ. Press, 2004
- [30] D. Bertsimas and J. N. Tsitsiklis, *Introduction to Linear Optimization*, vol. 6. Belmont, MA, USA: Athena Scientific, 1997.